*URSI GASS 2023, Sapporo, Japan, 19 – 26 August 2023*

# Armed Microstrip Patch: New Configuration with Promising Feature of High 3D Cross-Polar Discrimination

Debi Dutta* (1), Debatosh Guha (1)
(1) Institute of Radio Physics and Electronics, University of Calcutta India; e-mail:debidutta@ieee.org; dguha@ieee.org

## Abstract

This work explores a novel approach of controlling cross-polar (XP) radiations of a microstrip patch without tampering its ground plane or introducing any additional engineering. It proposes a new possibility where the patch geometry could be improvised without involving any expensive design or fabrication procedures. This, to the best of our knowledge, is the first of its kind which promises at least 10dB XP reduction over its diagonal plane without any rigorous feeding or structural engineering. The proposed geometry has also been experimentally tested and extended to realize improved array revealing equal amount of XP reduction over 3D radiation planes.

## 1 Introduction

There have been numerous techniques documented for enhancing cross-polar discrimination (XPD) of a microstrip antenna [1]-[3]. However, majority of them only focused to the principal (E- and H-) planes of radiation. But low XPD over the skewed planes i.e., around $\varphi \approx 45°$ to $70°$ is indeed a concerning issue for many antenna applications which has not yet been seriously addressed. Dubost [4] and Lee [5], [6] theoretically showed that XP radiation is a function of the azimuth angle ($\varphi$) having its maximum around diagonal (D-) plane i.e., $\varphi \approx \pm 45^0$. An article [7] revisited the same with the help of near field mathematical models to predict the variation of XP radiations over different $\varphi$-planes. Recently, Guha *et all* experimentally showcased the role of ground plane in controlling this D-plane XP issues [8], [9]. Ingenious current regulations were used there in by shaping of ground planes.

The present investigation addresses the same problem with a different as well as novel approach. It improvises the patch geometry itself and introduces loading by a pair of arms with an aim to controlling conduction current distribution. Two different configurations have been tested and the best possible design has been identified.

The idea is further prospected for making a representative 1×4 element H-plane array. The standalone version gives nearly 7 dB improvement in XP level over D-plane and 15dB in H-plane whereas the 4 element array shows remarkable improvement of about 10~12 dB in both planes. This eventually results the overall 3D XPD level of the proposed array around 30dB. In adaptive arrays where scanning over a wide azimuth range is necessary, consideration of the polarization purity in three-dimensional (3D) plane is a fundamental need [10].

The proposed design, therefore, should meet the requirements of antennas used in Synthetic Aperture Radar (SAR), polarimetric weather radar, and alike ones

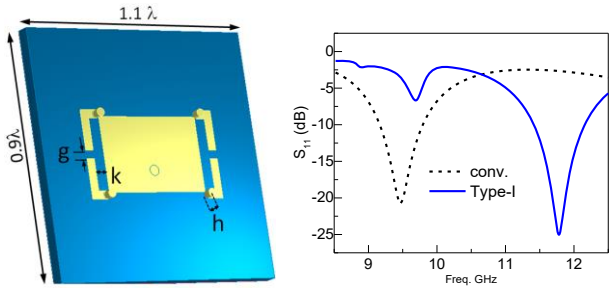


(a) (b)

Fig. 1. Proposed microstrip patch (Type-I configuration); (a) schematic diagram, (b) $S_{11}$ graph. Parameters are as $l_P = 9$, $w_P = 13.5$, $h = 2.575$, $g = 1.03$, $k = 1.44$. All dimensions are in mm.

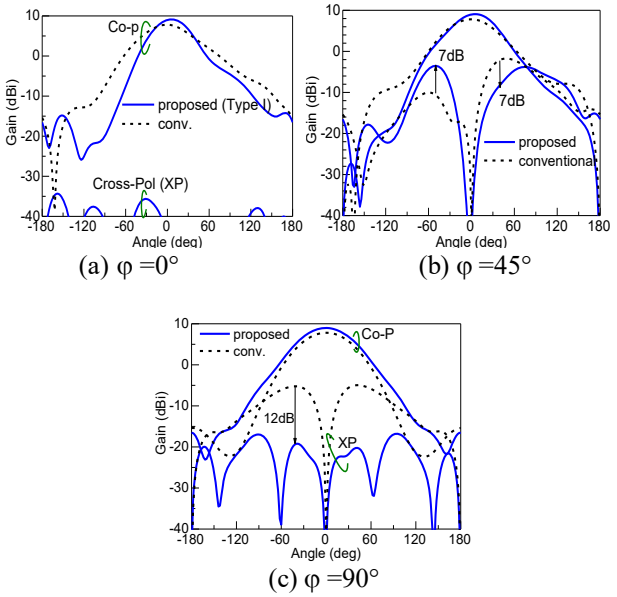


(a) φ =0° (b) φ =45°

(c) φ =90°

Fig. 2. Simulated radiation characteristics using [10] of Type-I configuration in resonance frequency; (a) E-plane, (b) D-plane, (c) H-plane

The proposed design, therefore, should meet the requirements of antennas used in Synthetic Aperture Radar (SAR), polarimetric weather radar, and alike ones

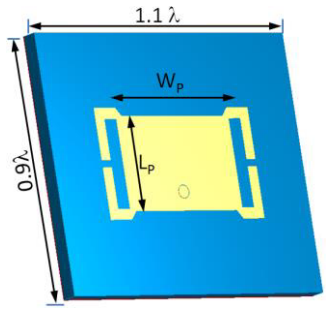


Fig. 3. Proposed pin and stub loaded planar microstrip patch (Type II). Parameters are as $l$ = 9, $w$ = 13.5, $h$ = 2.575, $g$ = 1.03, All are in mm.

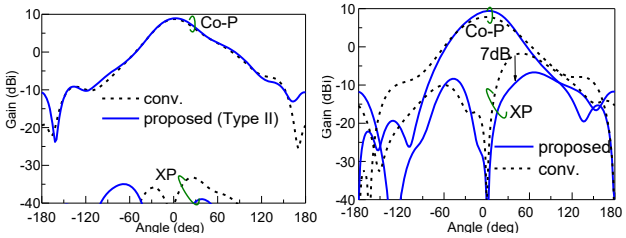


(a) φ =0° (b) φ =45°

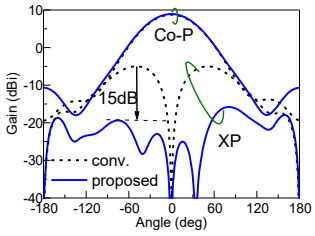


(c) φ =90°

Fig. 4. Simulated radiation characteristics of Type-II configuration in resonance frequency; (a) E-plane, (b) D-plane, (c) H-plane.

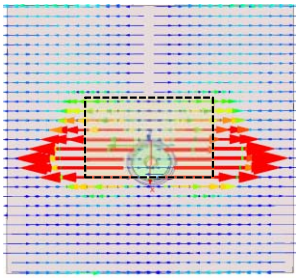

(a) Conventional: strong Jy

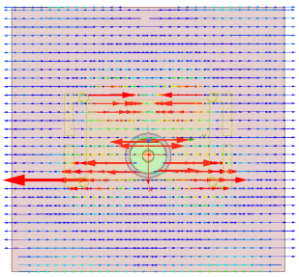

(b) Type-I (reduced, little unbalanced $J_y$)

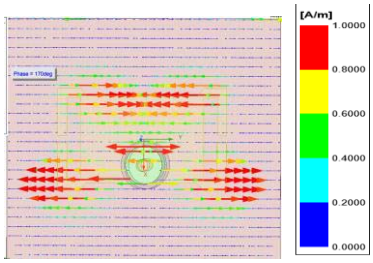


(c) Type-II (reduced, balanced $J_y$)

Fig. 5. Simulated Portray of $J_Y$ (A/m) on ground for (a) conventional, (b) Type-I and (c) Type-II configurations. Scale(0-1 A/m)

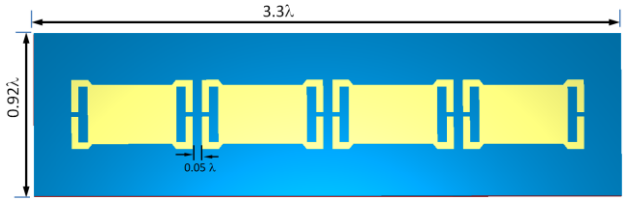


Fig. 6. Schematic view of proposed 1×4 element array with Type-II configuration.

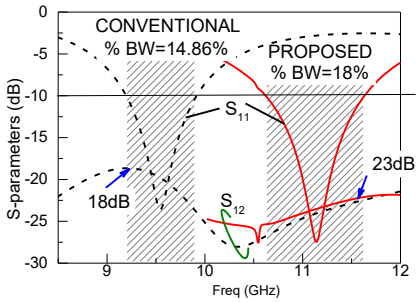


Fig. 7. Simulated $S_{11}$ and $S_{12}$ characteristics of array as shown in Fig. 6.

polarization purity.

## 2 Design and Performance

The antenna under investigation is a coax-fed microstrip element realized on 62mil RT/Duroid 5870 substrate to operate in X-band. Two configurations have been proposed and studied in steps.

### 2.1 Type-I configuration

This geometry is shown in Fig. 1(a). Small shorting pins have been inserted at four corners. In addition, two pairs of planar arms have been introduced as shown in the figure. Each pair embodies two folded arms with an intermediate gap and their cumulative dimension is of the order of λ/2, excluding the gap 'g'. This configuration indeed modifies the boundary condition of a typical microstrip patch and hence redistributes the overall patch current. This is reflected in Fig. 1(b) which compares the $S_{11}$ characteristics of the proposed one with its conventional counterpart. The resonance considerably shifts to higher frequency sides indicating its effective length relatively shorter or a kind of inductive loading caused by the shorted arms. The radiation of this new antenna, depicted through Fig. 2, appears quite interesting. The peak gain increases by about 1.5dB with an indication of selective suppression of backside radiation by as much as 5dB. Most interestingly, its XP radiation significantly decreases over H-plane but not revealed over D-plane. The D-plane XP follows a pattern which appears just reverse to that occurring in a conventional geometry. This shortcoming demands

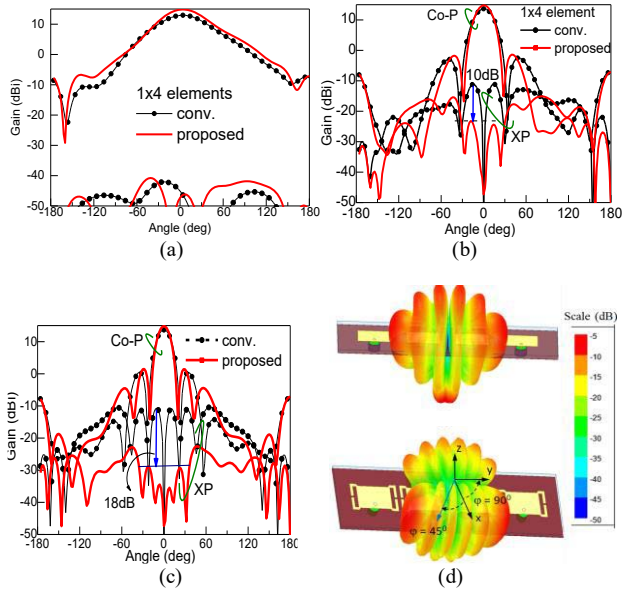


Fig. 8. Simulated gain pattern of proposed array (Fig. 6) (a) E-plane, (b) D-plane, (c) H-plane, (d) 3D view of XP fields (up: conventional, down: proposed)

further investigations especially in view of improving the D-plane scenario.

## 2.2 Type-II configuration

The above mentioned limitation of earlier configuration-I leads to a new variant, termed as configuration-II as shown in Fig. 3. This bears floating arms without any shorting by vias. The same trend of right shift of resonance frequency is found. However, the proposed configuration successfully suppresses the XP level in D-plane by 7dB (Fig. 4(b)) and the same in H-plane by 15 dB (Fig. 4(c)). No major change or distortion is found in the co-polarized radiation.

Low XP in D-plane can be realized by viewing the y-polarized ground plane current ($J_Y$), since it is related with D- and H- plane (φ = 45°, 90°) XP fields as [7], [8]:

$$XP(\theta)_{\varphi=45} \propto \iint \{J(y)[1+\cos\theta] - J(x)[1-\cos\theta]\} e^{j\beta \acute{r}.\hat{r}}\, d\acute{s} \quad \ldots(1)$$

$$XP(\theta)_{\varphi=90} \propto \iint 2\,J(y) e^{j\beta \acute{r}.\hat{r}}\, d\acute{s} \quad \ldots(2)$$

A set of simulated portrays of $J_Y$ components have been plotted in Fig. 5. The reference microstrip shows quite strong $J_Y$ distribution over its ground whereas both Type-I and Type-II reveals comparatively weaker $J_Y$. Moreover an additional phase reversal of $J_Y$ is found at the patch corners where the arms are located. This is true for both shorted (Type-I) and floating (Type-II) arms. The modified $J_Y$ takes part in generating low XP radiations in both the planes. Type-I pattern reveals little unbalance phase reversal whereas Type-II produces a uniformly balanced view of the same. This distribution eventually

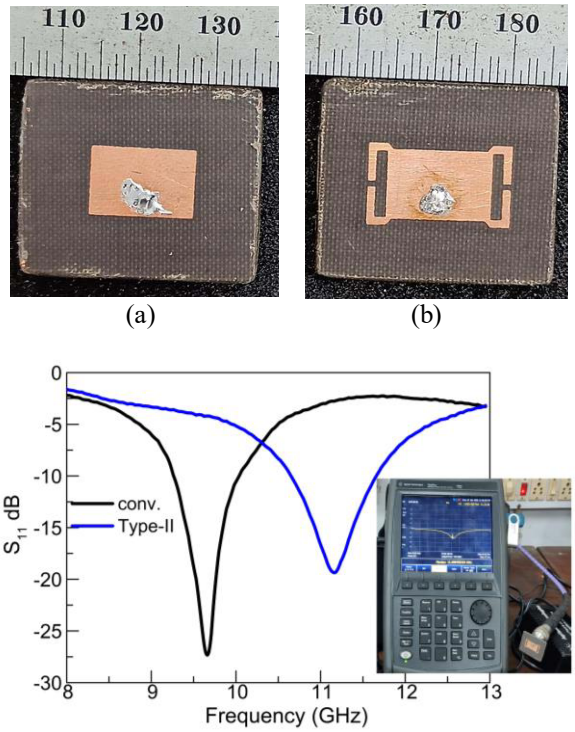


Fig. 9. Photograph of the prototype, (a) conventional, (b) Type-II patch. Parameters are as: *GL*=25, *GW* = 30, $l_P$ = 9, $w_P$ = 13.5, *g* =1.03 mm, *h* =1.575. All dimension in mm. (b) Measured $S_{11}$ values of for conventional and proposed prototype.

helps to realize the specific nature of D-plane XP for both the proposed configurations.

## 3 Feasibility of Array Design

The studies and observations so far were concentrated on the suppression of XP fields in both the D- and H- plane. This eventually improves the overall 3D cross-pol discrimination (XPD) of the single unit. This section investigates whether the same approach in Type II antenna can perform well for an array version.

Fig. 6 represents a 1×4 H-elements compact array bearing similar corner stubs as in Fig. 3. The inter element distance is kept ~ 0.05$\lambda_0$; $\lambda_0$ is the free space wavelength. Its performance has been compared with a conventional 1×4 H-plane array of similar shape and size through Figs.7-8. The $S_{11}$ curve (Fig. 7) for the proposed array shows a 'dip' at 11.10 GHz whereas the resonance frequency for conventional is found at 9.5GHz. Nearly 1.5 GHz right shift occurs due to insertion of those additional current carrying arms. The port-to-port isolation has been improved by 5dB along with 4% increment in operational bandwidth. Fig. 8 presents their radiation pattern in three principal planes. Peak gain has been increased nearly by 2dB in the proposed configuration. A remarkable achievement is found in the D-plane XP level which has been adequately suppressed by 10dB. The H-plane XP

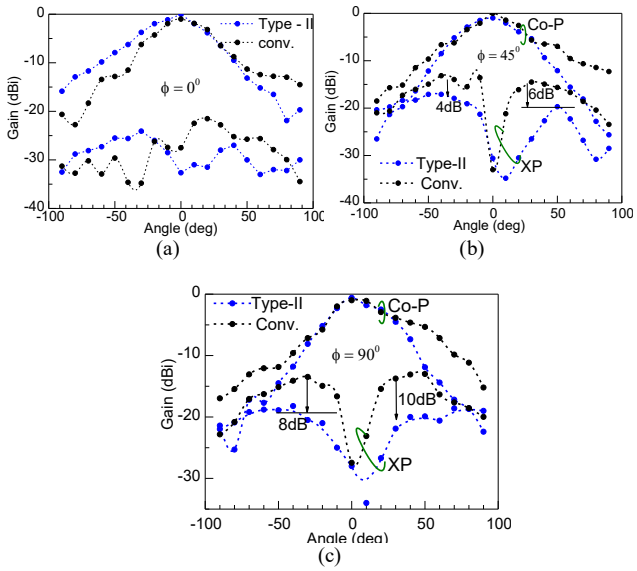


Fig. 10. Measured radiation characteristics of the prototypes: (a) E-plane, (b) D-plane, (c) H-plane.

radiation is also found to be suppressed by 18dB. This eventually improves the overall 3D polarization purity of the proposed probe-fed array by about 10-12dB. A comparative view of 3D XP distribution can be visualized from Fig. 8(d).

## 4 Experimental Validation

Figure 9 (a-b) depicts the prototypes of the conventional and the Type II configurations. Fieldfox Vector Network Analyzer N9926A has been used to measure their $S_{11}$ values. Fig. 9 (c) examines their $S_{11}$ patterns. The resonance is found to be 9.5GHz for conventional and 11.08GHz for the proposed one. This right shift is caused by additional current paths as formed by the corner arms. Their radiation patterns in three principal planes i.e., E-, D- and H-planes have been measured using in-house laboratory measurement facility (Fig. 10). The measured data have been furnished up to $\pm 90^0$ elevation angle since our in-house experimental set up provides error free data up to that range. The measured co-polarized patterns for proposed antenna show reduced backside radiations compared to the reference patch. Moreover, significant reduction is revealed for both in the D- and H-plane by about 7 – 10 dB respectively. This result eventually helps in improving the 3D cross-polar discrimination (XPD) for the proposed antenna.

## 5 Table I

| Ref. | Reduction in XP (dB) | | Gain | Comment |
|---|---|---|---|---|
| | D-plane | H-plane | | |
| [1] | Not addressed | 15 | 8.5 | nonplanar |
| [2] | ” | 10 | 6.5 | planar |
| [3] | ” | 6-8 | 7.8 | planar |
| [9] | 11 (single)<br>5(array) | 16 | 9<br>14 | planar |
| present | 7 (single)<br>10(array) | 15<br>18 | 8.2<br>14 | planar |

## 6 Conclusion

This paper presents a simple but effective technique to mitigate the high XP issue of a probe-fed patch antenna in its skewed planes. This newly proposed design, both the single unit and its array appear to be much useful and practically viable compared to the earlier ones, as documented in Table 1.

## References


[1] D. Dutta, D. Guha, and C. Kumar, “Microstrip Patch with Grounded Spikes: A New Technique to Discriminate Orthogonal Mode for Reducing Cross-Polarized Radiations,” *IEEE Trans. Antennas Propag.*, 70, 3, pp. 2295-2300, Mar.2022.

[2] T. Sarkar, A. Ghosh, L. L. K. Singh, S. Chattopadhyay and C. -Y. -D. Sim, "DGS-Integrated Air-Loaded Wideband Microstrip Antenna for X- and Ku-Band," *IEEE Antennas Wireless Propag. Lett.*, 19, 1, pp. 114-118, Jan. 2020

[3] C. H. Lai, T. Y. Han, and T. R. Chen, “Broadband aperture-coupled microstrip antennas with low cross polarization and back radiation,” *Prog. Electromag. Research Lett*., vol. 5, 187-197, 2020.

[4] G. Dubost, “Far field radiated by rectangular patch microstrip antenna,” *Electron. Lett.*, 18, 23, Nov.1982.

[5] T. Huynh, K. F. Lee, and R.Q. Lee, “Cross polarization characteristics of rectangular patch antennas,” *Electron. Lett.*, 24, 8, pp. 463- 464, Apr. 1988.

[6] K. F. Lee, K. M. Luk, and P. Y. Tam, “Cross polarization characteristics of circular patch antenna,” *Electron. Lett*., 28, 6, pp. 587-589, Mar. 1992.

[7] S. Bhardwaj and Y. Rahmat-Samii, “Revisiting the generation of crosspolarization in rectangular patch antennas: A near-field approach,” *IEEE Antennas Propag. Mag.*, 56, 1, pp. 14-38, Feb. 2014.

[8] D. Dutta, S. Rafidul, D. Guha, and C. Kumar, “Suppression of crosspolarized fields of microstrip patch across all skewed and orthogonal radiation planes,” *IEEE Antennas Wireless Propag. Lett*., 19, 1, pp. 99-103, Jan. 2020.

[9] S. Rafidul, D. Guha, and C. Kumar, "Sources of Cross-Polarized Radiation in Microstrip Patches: Multiparametric Identification and Insights for Advanced Engineering," *IEEE Antennas Propag. Mag.*(early access), doi: 10.1109/MAP.2022.3143434.

[10] A. H. Aljuhani, T. Kanar, S. Zihir, and G. M. Rebeiz, "A 256-Element Ku-Band Polarization Agile SATCOM Transmit Phased Array With Wide-Scan Angles, Low Cross Polarization, Deep Nulls, and 36.5-dBW EIRP per Polarization," in IEEE Transactions on Microwave Theory and Techniques, vol. 69, no. 5, pp. 2594-2608, May 2021.